

Prepared for the
National Institutes of Health
National Institute of Neurological Disorders and Stroke
Neural Prosthesis Program
Bethesda, MD 20892

**ELECTRODES FOR FUNCTIONAL
NEUROMUSCULAR STIMULATION**

Contract #NO1-NS-32300

**Quarterly Progress Report #7
1 April, 1995 - 30 June, 1995**

**Principal Investigator
J. Thomas Mortimer, Ph.D.**

**Co-Investigator
Warren M. Grill, Ph.D.**

**Applied Neural Control Laboratory
Department of Biomedical Engineering
Case Western Reserve University
Cleveland, OH 44106**

This QPR is being sent to
you before it has been
reviewed by the staff of the
Neural Prosthesis Program

Table of Contents

	page
B. Electrode Design and Fabrication	
B.2 Electrode Testing: Corrosion Testing of Cuff Electrodes	3
C. Assessment of Electrode Performance in an Animal Model	
C.1.b Performance Testing in Chronic Animal Experiments	33
Appendix I: Manuscript	34

Section B: Electrode Design and Fabrication**B.2 Electrode Testing: Corrosion Testing of Cuff Electrodes****Abstract**

To investigate their resistance to corrosion, three 12-contact spiral cuff electrodes were stimulated continuously for 10 weeks while submerged in individual flasks containing phosphate buffered saline solution. Microscopic analysis of the contacts of the cuffs has been completed. Stimulation related effects were found on those contacts stimulated at higher than anticipated charge densities. The welds between the lead wires and the platinum contacts were also examined microscopically. The condition of the platinum contacts, in both stimulated and unstimulated regions, as well as the condition of the weld zones, is summarized.

Previous Work

In previous progress reports (QPR #4 and #5), the experimental set-up and measurements made over the 10 week period were presented in detail. Briefly, three multiple contact spiral nerve cuff electrodes were immersed in individual flasks of saline solution and stimulated continuously for ten weeks. The contacts were stimulated with 0 (control), 1, 2, and 3 mA amplitude balanced charge rectangular pulses, with 50 μ s pulsewidth, at a frequency of 20Hz, and with a recharge limit of approximately 300 μ A. Potential measurements made over the course of the stimulation were presented in QPR #5. A schematic of the cuffs and the stimulation of each contact is presented in Figure 1.

After removing the cuffs from the flasks of saline, they were initially examined using a low power dissecting microscope. To further investigate, the contacts of each cuff were cut out of the silicone rubber sheeting and prepared for SEM examination. Contacts from Cuff A were examined first and were found to have significant amounts of adherent debris which obscured much surface detail. The contacts from the remaining cuffs, Cuff B and C, were sonicated in solutions of Liquinox and ethanol before mounting on SEM stages.

Initial microscopic analysis of the contacts and their welds was presented previously (QPRs #5 and #6). This analysis has been completed, and summarized results are discussed here.

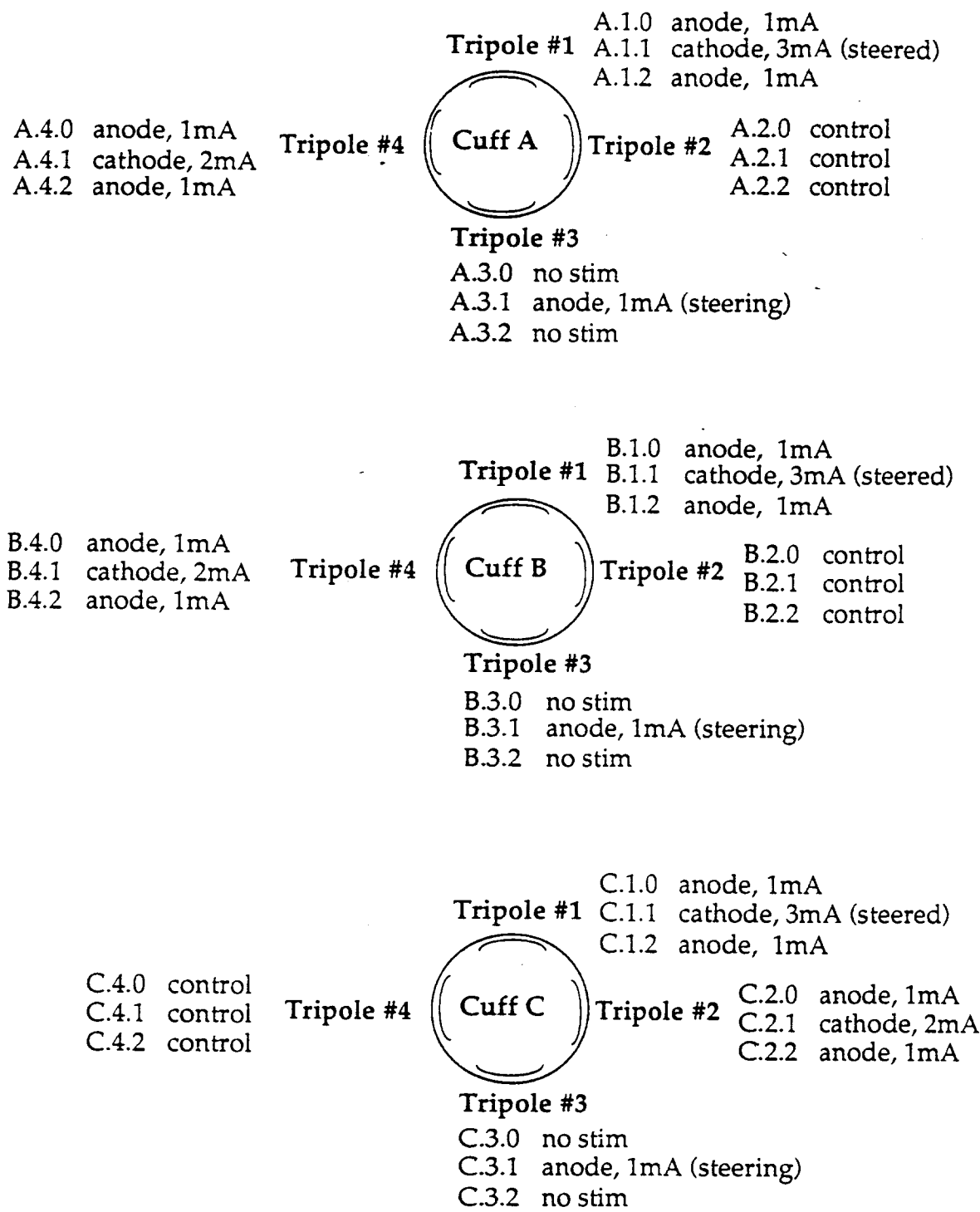


Figure 1: Cross-sectional schematic of the cuffs, with the stimulation and amplitudes of each contact indicated.

Examination of Contacts

After having been cleaned, mounted on aluminum stages, and sputter coated with approximately 200Å thick gold plating, the contacts from each cuff were examined using a Scanning Electron Microscope (SEM). The face of the contact was examined initially, and then the contacts were flipped over so that the weld and the back side of the contact could be examined. Attention was focused on those areas in the exposed stimulating region and in the weld zones, however, all areas of the contact were examined. Any observed surface phenomena were further examined at higher magnifications.

Fabrication Process

In making spiral cuff electrodes, the contacts are hand cut out of a sheet of platinum foil 35µm thick using a scalpel or razor blade. Nominal size for the contacts is 1.0 mm on a side. The lead wires are then spot-welded to one side of the contact. The contacts and attached lead wires are placed between sheets of silicone rubber and a layer of silicone elastomer and cured in a press, in this case to a nominal total thickness of 350 µm. A window is cut in the top layer of silicone to expose a 0.7 mm diameter circular area in the center of the platinum contact. In these fabrication steps, the potential exists for damage to the platinum foil and the creation of inconsistencies between contacts, both of which may increase vulnerability to corrosive attack and other types of failures.

General Condition of Platinum Contacts

Observations of the general condition of the platinum foil contacts were made during this evaluation of the in vitro cuffs and are discussed below. It has been apparent that the hand fabrication procedure is cumbersome, is prone to variation in cuff quality, and has room for many improvements. In evaluating these contacts, the damaging effects of some of the current fabrication procedures were observed and should be considered when developing improved fabrication techniques.

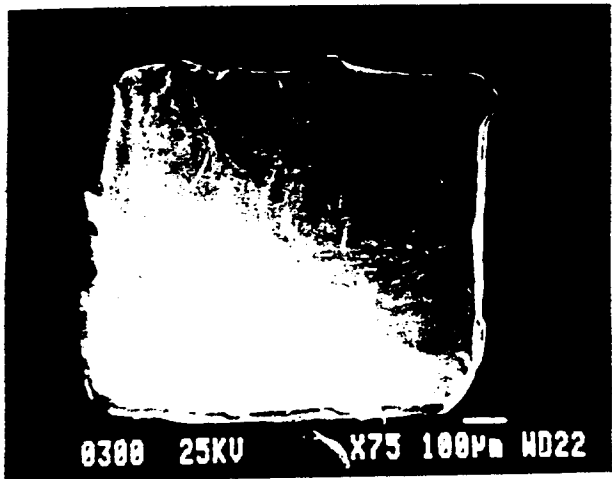
Size and Shape of Contacts

Based on SEM photographs, the size of the contacts ranged from 0.56 - 1.30 mm² (0.7 × 0.8 mm to 1.0 × 1.3 mm), where 1.0 mm² was nominal. Once extracted from the silicone rubber sheeting, many of the contacts exhibited an inherent curl, likely due to their position inside of the curled, spiral cuff. To avoid creating damage to the contact, no attempts were made to completely flatten the foil. Therefore, size was estimated where curl of the contact was present.

The contacts were found to be generally square, with the lengths of a side of a single contact differing by an average of only 0.13 mm, but in one case being as high as 0.4 mm. In addition to some non-uniformity in size of the contacts, the effects of hand cutting the pieces were seen by excess or missing platinum at corners and by small ridges or lips along the edge (Figure

2). These most likely occurred due to inadequate cutting of the contact, although handling and even the press curing may have contributed.

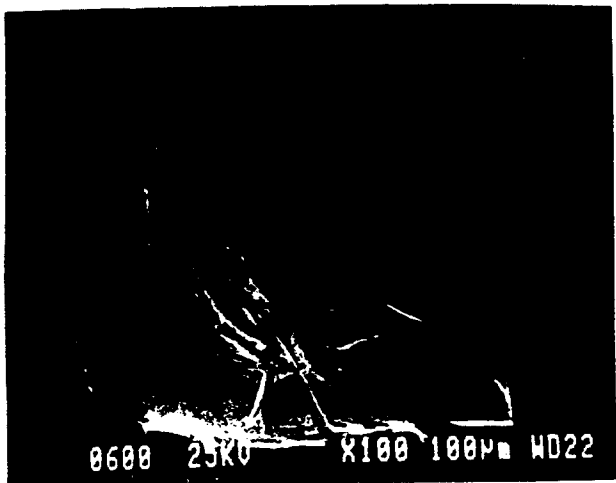
Size and Shape of Contacts



2.a: Photomicrograph of contact B.2.0



2.b: Photomicrograph of contact C.3.0



2.c: Photomicrograph of contact B.3.1



2.d: Photomicrograph of contact A.3.1

Figure 2: SEM photomicrographs demonstrating the effects of hand cutting the platinum contacts. Excess platinum is evident in 2.a, while missing platinum is evident in the lower right corner of 2.b. Ridges and tear marks are seen along the edges of 2.c and 2.d.

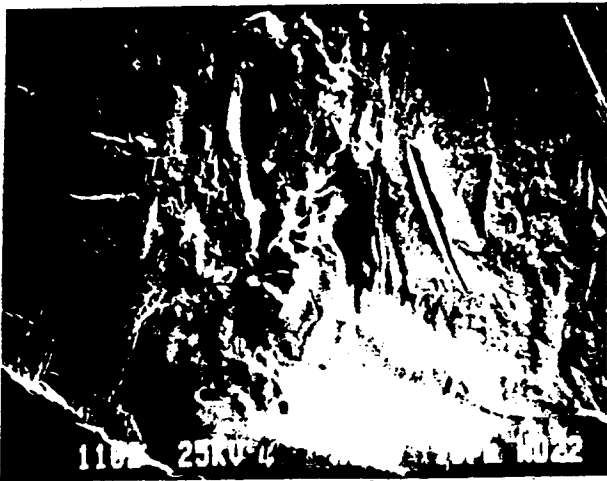
Effects of Spot Welding

The spot welding is performed on the back side of the contact between the platinum foil and the stainless steel lead wires. The welds themselves are discussed in a following section, but some effects of the welds could be seen on the front face of several contacts and are discussed here. In addition, there appeared to be some evidence of welding on the front face that was not related to the weld zone on the back side. These may be instances where an attempt was made to create a weld, the attempt was a failure, and the contact was then flipped over to be successfully welded on the other side, leaving weld marks on the face.

In direct association with the weld zone on the back side, distortions and voids were found on the faces of 4 contacts. The distortions, seen on two different contacts, are in areas where excessive heat was likely generated during the weld. In one case, the distortion overlies a large weld nugget (Figure 3.a, 3.b). In the other instance, the distortion overlies an area that appears to contain some weld metal (Figure 3.c, 3.d), probably originating from a failed weld attempt. The voids with the very round shape, as shown in Figure 3.a appear to indicate gas escape. In other cases, the voids were irregular in shape and appear to be from inclusions or other metallurgical origins (Figure 4). A small slit was also found in the interior of another contact overlying the weld area, as shown in Figure 5, but the view of the weld does not clearly indicate the weld as the source of this slit.

In 3 contacts, isolated spots similar in appearance to weld areas were found on the face, but examination of the back side revealed no corresponding weld in that area. On a single contact, a void, similar in appearance to a large inclusion site was found in close proximity to a circular area exhibiting disturbed surface morphology, as presented in Figure 6.a. The well-defined border of this circular area and the difference in surface appearance in this area point to an artificially induced defect, likely the welding electrode tip. The electrode tip may also have been the cause of the defects shown in Figure 6.b and 6.c, whose appearance and circular shape resembles that of some of the weld zones seen on the back sides. If misaligned over the lead wire, the electrode tip can press directly onto the platinum foil during a spot welding attempt, leaving behind residual electrode metal and altered metallurgy of the platinum, but obviously no weld between the wire and the foil. If this occurred, or if for any other reason a weld was not adequate, the contact may have been turned over to be welded on the other side.

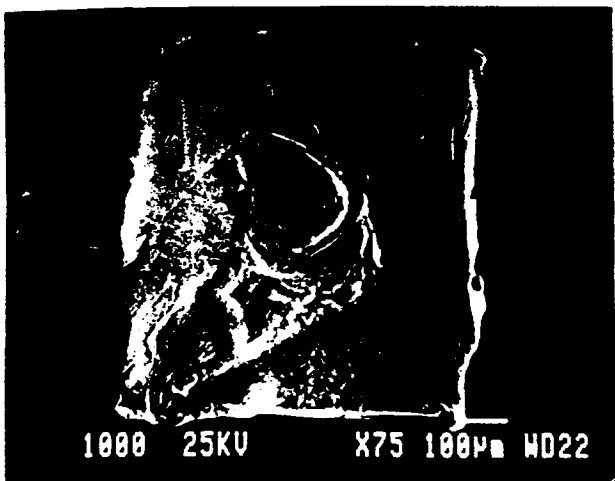
Distortions and Voids from Weld Zones



3.a: Photomicrograph of contact C.3.2



3.b: Photomicrograph of contact C.3.2



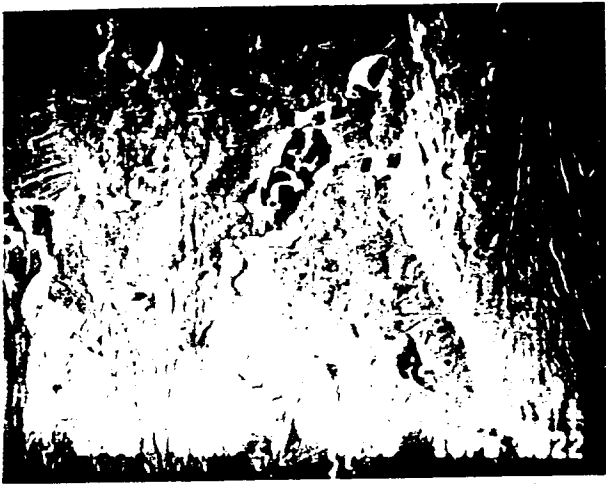
3.c: Photomicrograph of contact B.3.2



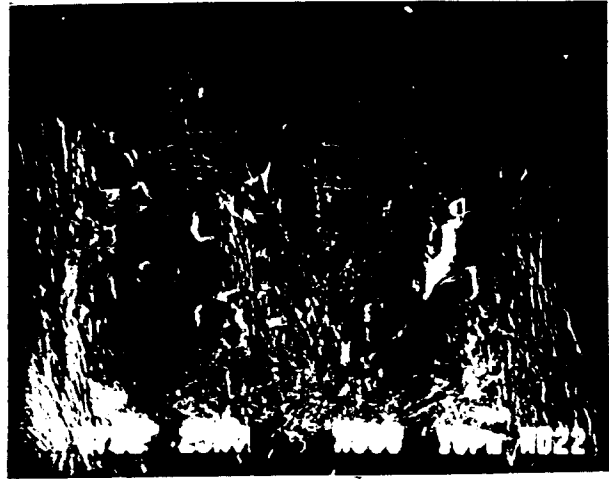
3.d: Photomicrograph of contact B.3.2

Figure 3: SEM photomicrographs representing distortions and round voids overlying weld zones. The front face is presented in 3.a and 3.c, while the back faces are shown in 3.b and 3.d. The distortion seen in 3.a overlies the large weld nugget shown in 3.b. The hook-shaped distortion seen in the lower left corner of 3.c can also be seen in 3.d in an area of weld metal.

Voids from Weld Zone



4.a: Photomicrograph of contact B.2.1



4.b: Photomicrograph of contact B.2.1

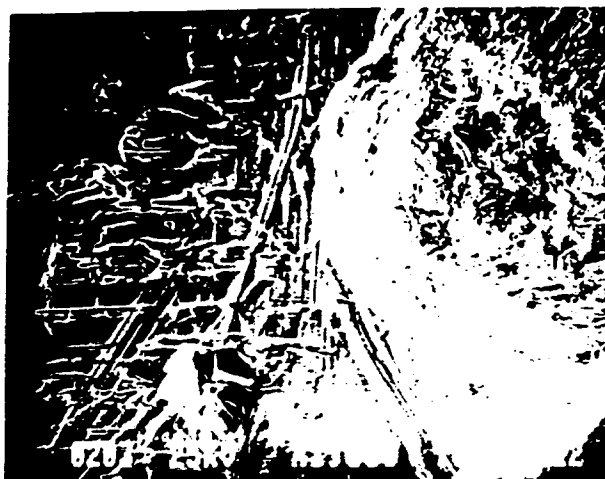
Figure 4: SEM photomicrographs of inclusion voids seen in areas overlying weld zones.

Slit in Area of Weld Zone



Figure 5: SEM photomicrograph of contact C.4.2. The slit is in the area of the weld, although the view of the back side does not provide conclusive evidence that the weld was the source.

Weld Marks on Face of Contacts



6.a: Photomicrograph of contact C.2.0



6.b: Photomicrograph of contact B.1.2



6.c: Photomicrograph of contact C.2.1

Figure 6: SEM photomicrographs of weld effects seen on the front face of the contact that were not related to the weld zone on the back side. The defect in 6.c is slightly above and left of center.

Effects of Press Curing

As part of the fabrication procedure, the cuff assembly is placed in a press to cure and bond the silicone rubber sheeting and elastomer together, incorporating the contacts and the lead wires. Spacers are used to create a desired nominal thickness, which in this case was 350 μ m. The sheeting for these cuffs totaled 250 μ m, the deinsulated wire has a minimum thickness of 35 μ m but the insulated wire has a thickness of 255 μ m, the platinum foil is 35 μ m thick, and the elastomer fills in the thickness around the wire and the contacts between the layers of sheeting. Even if just the sheeting and the insulated wire are considered, these elements of the cuff are thicker than the total thickness of the completed cuff, indicating that some compression occurs during the press curing. The silicone rubber sheeting and elastomer, due to their soft nature, are likely elements to absorb some of this compression. Platinum is a very soft metal and examination of these contacts revealed that many of the platinum foil pieces were effected physically by the presence of the wires behind them, likely generated as they were pressed together.

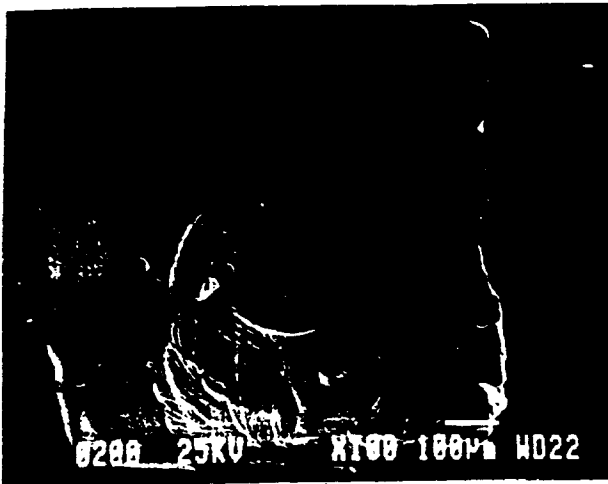
In roughly two thirds of the contacts, the presence of the lead wires could be readily observed on the front face of the contact. In most of these cases, an outline of the wire group or of individual strands was distinguishable on the face of the contact, as if the wire(s) had started to press through the platinum foil. This is demonstrated in Figure 7.a-d.

On several contacts, the surface morphology of the platinum foil was distinct in the area overlying the wire. A striated, cross-hatched pattern was seen on the surface. This is presented in Figure 8, and was confirmed to be in the region of the wires by examination of the back side of the contacts. These striations do not appear to correlate with the area of the welds.

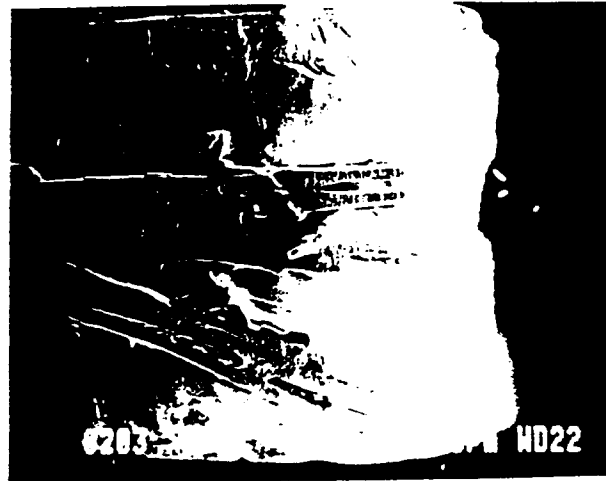
Finally, in two instances, actual tears in the platinum foil were created by the wires, as shown in Figure 9.a-d. These appear to have been created as the wire pressed entirely through the contact, and are clearly seen by the photographs taken on the back side of the contact where the position of the wire in relation to the tear is shown.

Press curing of the cuff, including all of the elements that make up the cuff, is set to a desired, minimal thickness. This 'minimal' thickness is calculated based primarily on the thickness of the layers of silicone rubber and is kept to a minimum to ensure proper bonding between layers. A thinner cuff is also desirable for implantation purposes. However, as the photomicrographs presented here show, care must be taken to avoid pressing the cuff too thin and ripping through the contacts with the wires.

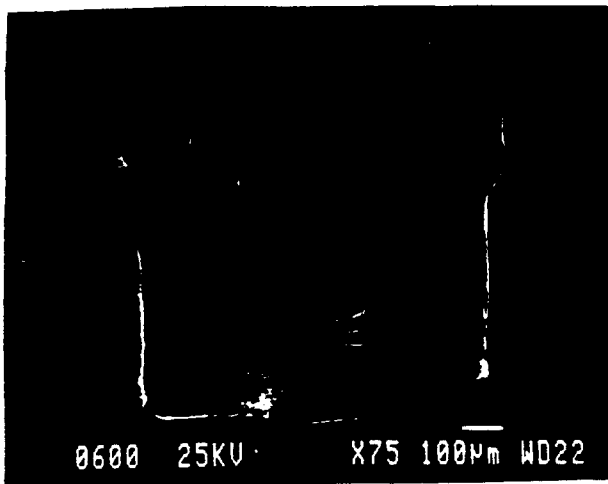
Effects of Press Curing



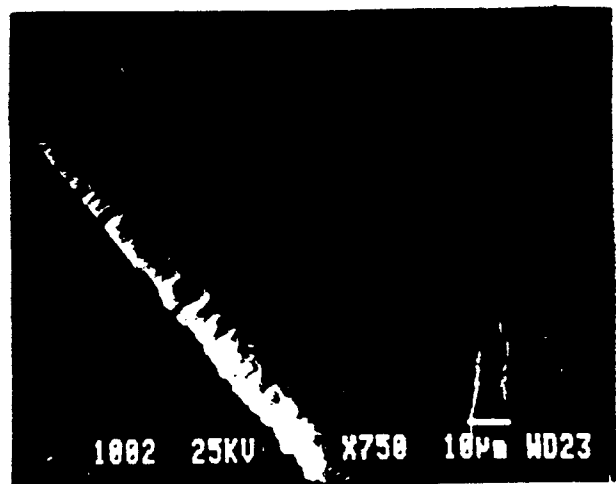
7.a: Photomicrograph of contact B.3.0



7.b: Photomicrograph of contact B.3.0



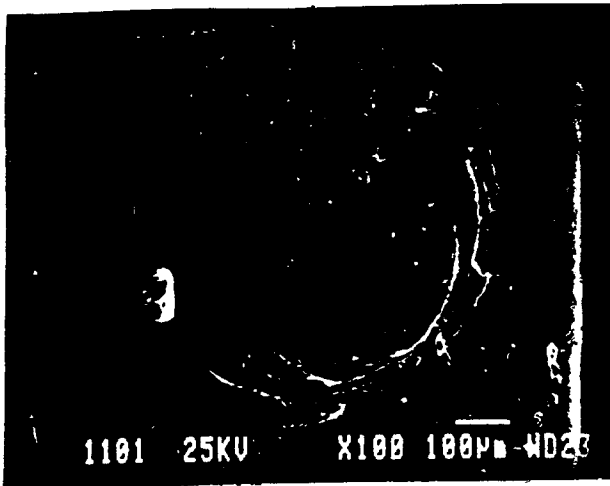
7.c: Photomicrograph of contact C.2.1



7.d: Photomicrograph of contact C.2.2

Figure 7: SEM photomicrographs showing the outline of wires as they dent the platinum foil contacts. The wire is particularly evident in 7.a along an upwards diagonal extending from the left edge that correlates with the wire strands on the downward diagonal in 7.b. An outline of the wires can be seen in the upper half of 7.c. A view of the impression made by a single wire strand on the backside of the contact is shown in 7.d.

Effects of Press Curing



8.a: Photomicrograph of contact A.3.2



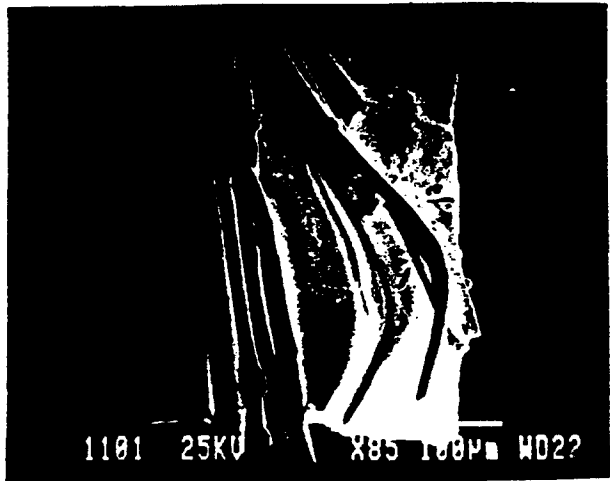
8.b: Photomicrograph of contact A.3.2

Figure 8: SEM photomicrographs of the striations and cross-hatching seen on some contacts in the area overlying the wires. 8.b is a higher magnification view of 8.a. Some surface debris can be seen in these photos.

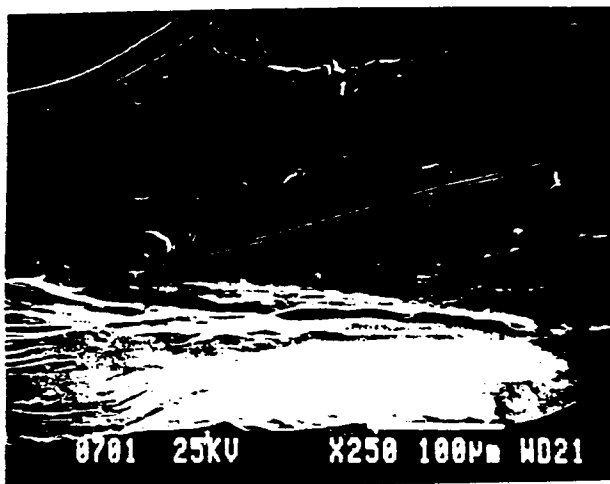
Effects of Press Curing



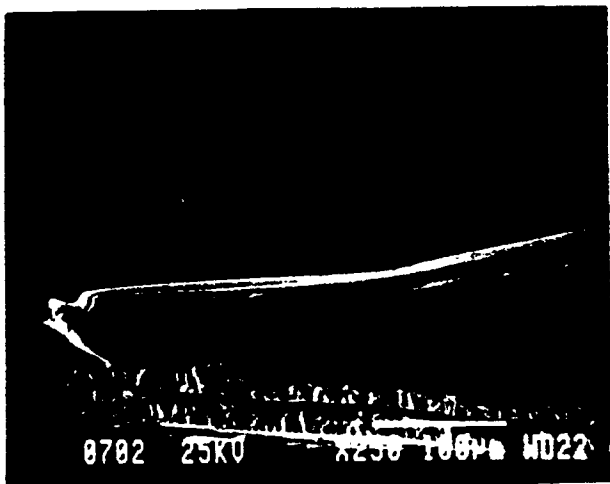
9.a: Photomicrograph of contact C.3.2



9.b: Photomicrograph of contact C.3.2



9.c: Photomicrograph of contact C.3.1



9.d: Photomicrograph of contact C.3.1

Figure 9: SEM photomicrographs of the two instances where the wires apparently tore through the platinum foil. A tear is seen in the lower right corner of 9.a corresponding to the wire dent on the lower edge of the back side of the contact as shown in 9.b. The other case where a tear occurred is shown on the face in 9.c and on the back in 9.d.

Effects of Window Cutting

To expose the platinum contacts and create the sites for current flow, the silicone rubber overlying the platinum must be removed. Windows are cut through the top layer of silicone rubber using a sharpened section of hypodermic tubing with an internal diameter of 0.7 mm. The tubing is pressed onto the silicone rubber and twisted slightly to effectively cut through the compliant rubber.

The sharpened tip, however, can gouge the platinum foil, particularly as the tubing is twisted. This gouging was observed on the majority of contacts examined, as shown in Figure 10.a and 10.b. The gouging created by the window-cutting tool decreases the mechanical integrity of the contact and creates vulnerable sites for corrosive attack.

Multiple gouge marks were found on a number of contacts (Figure 10.c), indicating that more than one attempt was needed to create the window. This could lead to creating larger and/or non-circular windows. If the gouge marks are used to delineate the borders of the window, the window sizes for these cuffs ranged from 0.31-0.8 mm diameter, despite having been cut with a 0.7 mm diameter cannula. Size and shape of the window is important when considering both charge density and the field generated during stimulation. Smaller contact size leads to higher charge densities, making the contact susceptible to corrosion.

The windows are cut to be symmetric and in the proper location for the final cuff configuration. However, the pieces of platinum are not precisely spaced between the sheeting and in roughly half of these contacts, the windows were not centered on the platinum piece (as determined using the gouge marks as the window border, Figure 10.d). Especially for those contacts that were smaller in size (down to 0.7mm on a side), any offset of the window could place the edge of the contact within the window, again effecting charge densities. If the edge of the contact were within the window, this would also increase the likelihood of creating an ionic path to the back side where accelerated galvanic corrosion could occur between the platinum and stainless steel.

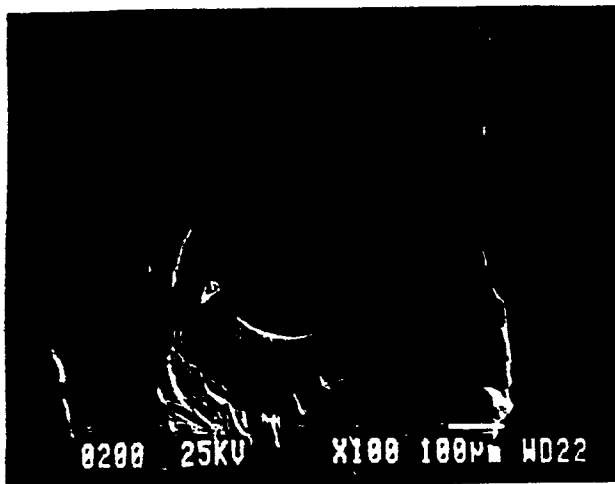
Effects of Window Cutting



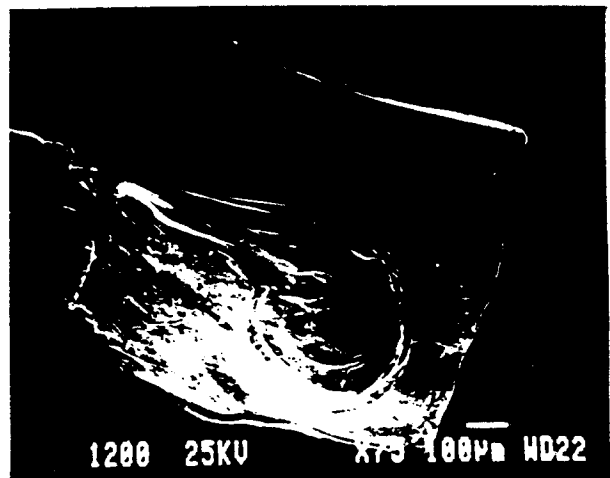
10.a: Photomicrograph of contact A.1.1



10.b: Photomicrograph of contact A.2.2



10.c: Photomicrograph of contact B.3.0



10.d: Photomicrograph of contact B.1.2

Figure 10: SEM photomicrographs representing the effects of the window cutting on the titanium foil. Excessive gouging is seen in 10.a and 10.b. Multiple gouges, which may have exposed a larger surface area, are shown in 10.c. In several contacts the window was offset from the center of the contact, as depicted in 10.d.

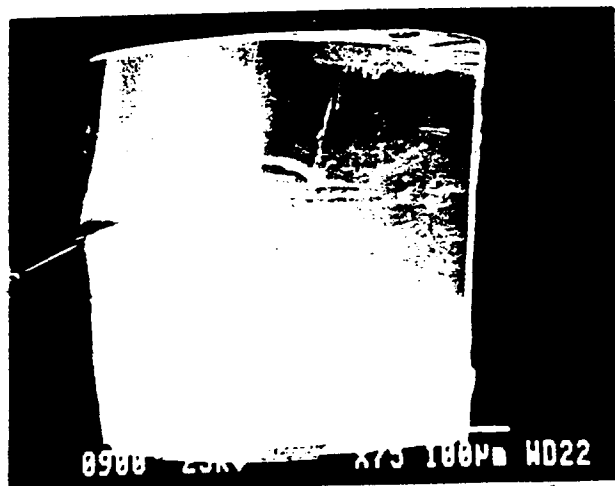
Effects of Curling of Cuff

Once fabricated, the spiral cuff electrode wraps around itself due to the stretched silicone rubber sheeting. The contacts are subjected to the curling as well, as they are embedded within the rubber sheeting. In the past, platinum foil measuring 5-10 μ m thick was used in the fabrication of spiral cuffs containing platinum bands, but the platinum was found to crack when bent. Therefore, thicker foil was required and 25-35 μ m thick foil is now used.

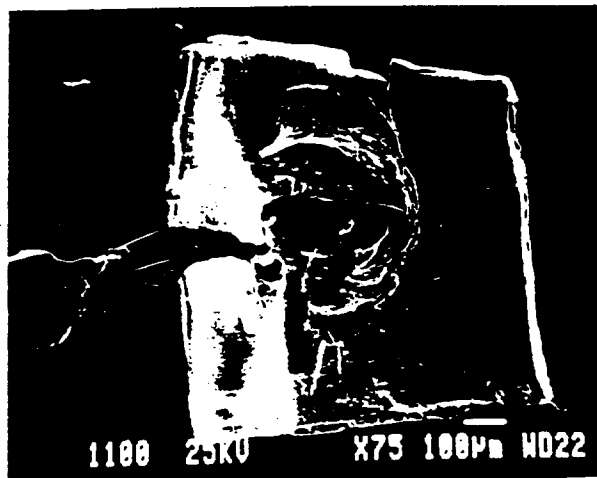
In these cuffs, 12 of the 36 contacts had cracks or tears, originating from the outer edge of the contact near the lead wire. In all instances, these cracks were found to be parallel to the line of the lead wires, which is perpendicular to the direction of the stretched sheeting, and hence, to the curl of the cuff. These cracks are represented in Figure 11.a-d.

Enough stress was placed on these pieces of platinum foil to create cracks. This stress may have originated with the curling of the cuff, particularly in those areas with the additional stiffness of the lead wire. It should be noted that these cuffs experienced some additional handling than might normally be experienced, both before and after the stimulation period. The possibility that this additional handling may have created cracks in the foil should be considered, particularly as preliminary examination of contacts in cuffs that were implanted *in vivo* for periods of over 6 months has found no cracks.

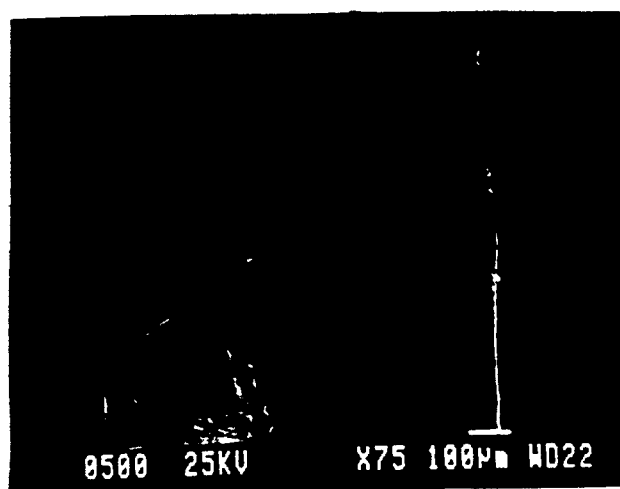
Effects of Curling of Cuff



11.a: Photomicrograph of contact C.1.2



11.b: Photomicrograph of contact B.2.2



11.c: Photomicrograph of contact C.1.1



11.d: Photomicrograph of contact C.1.1

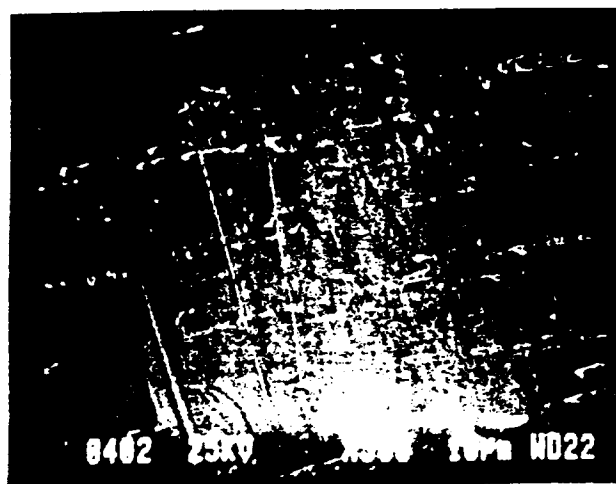
Figure 11: SEM photomicrographs representing the tears extending from the edge of the contacts. These tears run perpendicular to the direction of the curl of the contact and originate in the area of the lead wires. A higher magnification view of the crack shown in 11.c is presented in 11.d.

Metallurgical Defects

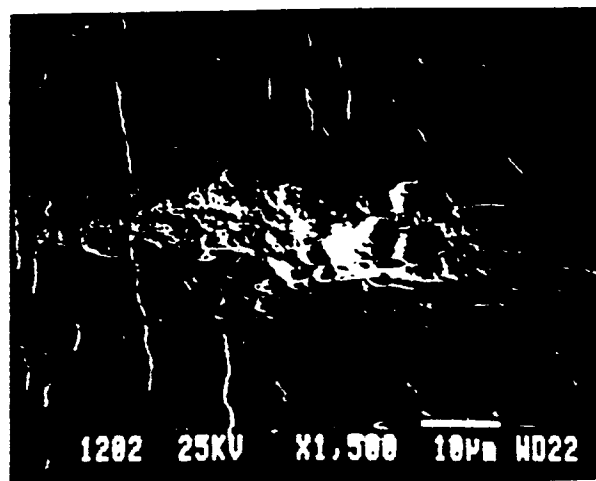
The platinum foil used as the contacts is purchased from Johnson Mathey or Goodfellow as pure platinum. However, this material may contain limited inherent flaws, as well as acquiring some defects during fabrication procedures. Several flaws were found in the contacts from these cuffs that are not apparently related to their stimulation, as they were observed on contacts that were not stimulated, and on both the unexposed and back surfaces of the foil pieces.

Lines of shallow pits were found on many contacts. These lines were primarily parallel to one another and extended in some instances for the entire length of the contact. These pit lines were also generally parallel to the edge of the contact and were found on the back sides of the contacts. Contaminant or defect created during the rolling of the sheet of foil may be responsible for these. Occasional diagonal lines containing shallow pits were also found on some contacts. Isolated pits and isolated regions of pits were seen in both exposed and unexposed regions of the platinum, as well as on the back sides. Examples of these defects are presented in Figure 12.a-d.

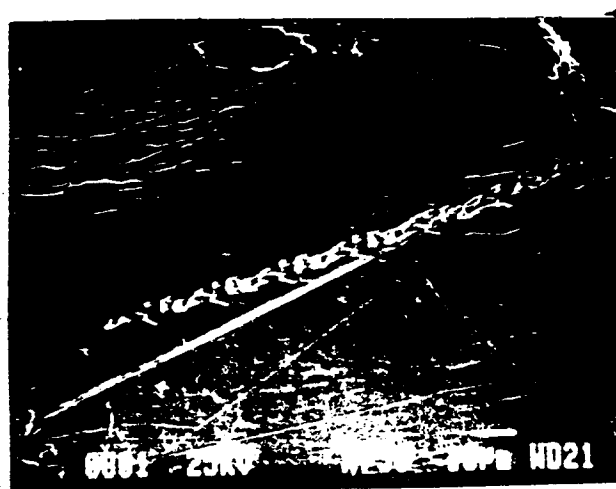
Metallurgical Defects



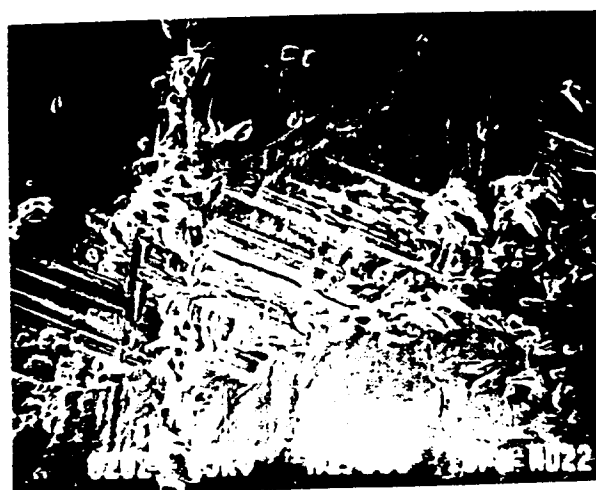
12.a: Photomicrograph of contact C.4.0



12.b: Photomicrograph of contact B.1.2



12.c: Photomicrograph of contact C.4.1



12.d: Photomicrograph of contact C.2.0

Figure 12: SEM photomicrographs representing the metallurgical defects found on the contacts. These defects were not correlated with either the exposed surface of the contacts, nor with the stimulation of the contacts.

Condition of Weld Zones

In fabricating these cuffs, multi-stranded 316L stainless steel wire is spot-welded under an argon atmosphere to one side of a piece of platinum foil. The current and pressure settings on the welder are adjustable, but are set within a predetermined range for welding the wire to the foil. The wire and foil are aligned under the weld electrode with the aid of a stereomicroscope. Using a foot pedal, the weld electrode is then lowered to press onto the wire and foil, completing the circuit path, and the weld members begin to heat through electrical resistance. Because of the size and number of wires to be welded, multiple weld spots may be required. Acceptable welds are determined based on visual appearance as determined by the welder.

The multi-stranded wire consists of 7 individual wires stranded together. When the insulation is removed, these strands tend to splay somewhat, which is beneficial as the diameter of the wire cable is then reduced. If the wire strands are splayed and lying entirely in a plane, their thickness is only 35 μm , instead of the 105 μm they encompass when stranded together. Dependent on the degree and location of splay, multiple weld spots may be required.

To evaluate the welds, the back sides of the contacts were examined using an SEM. In a few cases, the lead wire broke off of the contact either during extraction from the silicone rubber, or during handling and cleaning. When possible, the broken wire end was examined in addition to examination of the back face of the contact.

In the examination, the welds typically involved most of the wire strands. The histogram shown in Figure 13 demonstrates that of the 35 contacts where it was determinable, over two thirds of the contacts had 6 or more wire strands contained within a weld. These data show that despite a cumbersome process, the spot welding was generally successful at effecting most of the wire. In a visual examination, this would indicate to the welder that the wire was well bonded to the foil.

However, both wire strands and weld bonds were found to have failed. Broken wire strands were seen in areas adjacent to the weld in 6 different contacts, as represented in Figure 14.a-c. During the welding, the wire strands heat and the molten metal goes into the weld nugget. This leads to thinning of the wire strands in those areas, as shown in Figure 14.c-d, and subsequent reduced strength. When the contacts were extracted from the sheeting, tension was applied to the lead wire, which could have initiated wire strand breaks. However, some tension is also applied to the lead wires during fabrication, cleaning, etc., and may have played a role in these failures.

In four of the contacts, the weld bonds failed upon removing the contacts from the silicone rubber sheeting. Examination of the wire ends and the back side of the contacts reveals that two of these failures occurred where 4 wire strands were involved in the weld, one occurred where 6 strands were in the weld, and one occurred where all 7 strands were apparently welded.

Platinum is an excellent electrical conductor with very low inherent resistivity. During welding, the weld pieces are intended to be heated due to their electrical resistance so that they become molten, mix together and form a metallurgical bond. Because of its lower resistance, the platinum heats slower than the stainless steel. The configuration of the weld electrodes also promotes additional heating of the stainless steel. In these cases of de-bonding, it would seem that an adequate weld was never established between the platinum foil and the stainless steel wire strands. A likely cause is inadequate heating of the platinum foil. The photomicrograph presented in Figure 15 shows the back side of a contact where the weld bond failed. No evidence of the weld could be seen on the surface of the platinum.

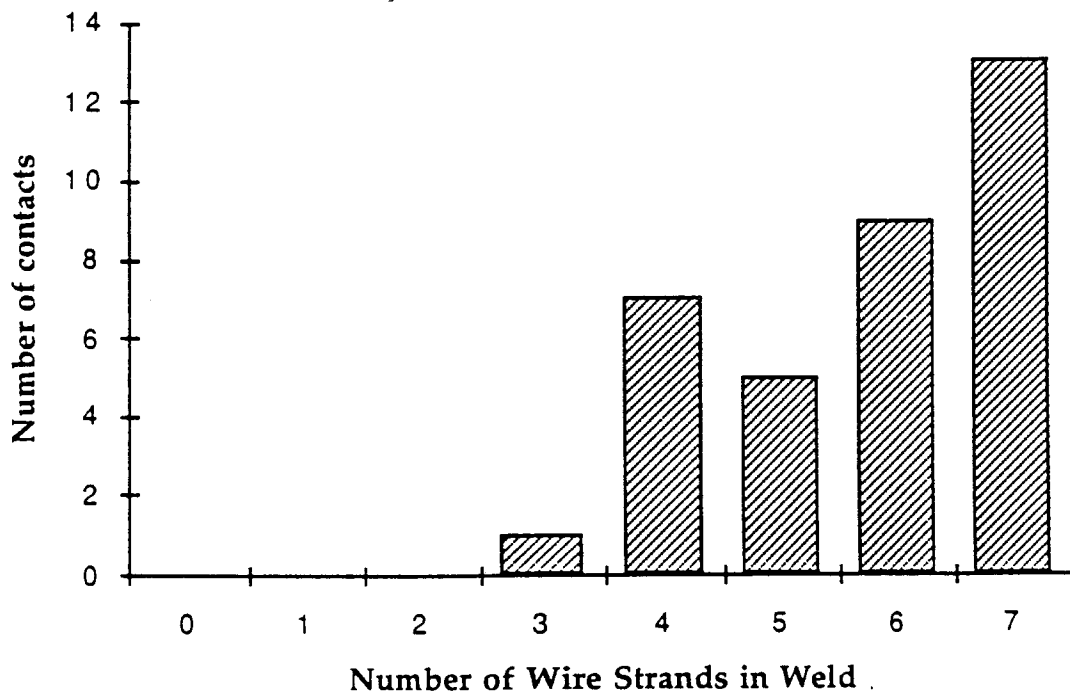
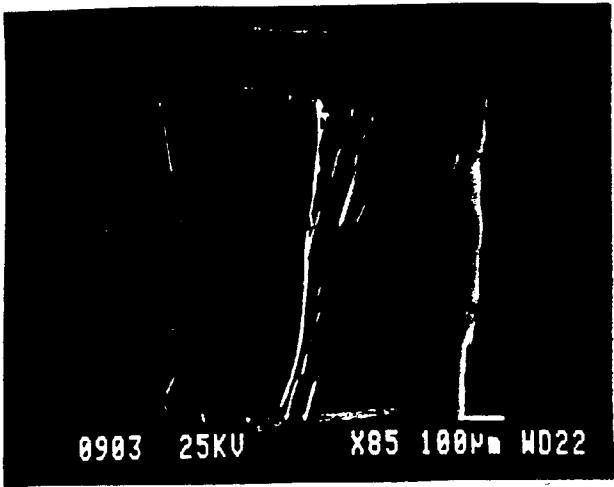
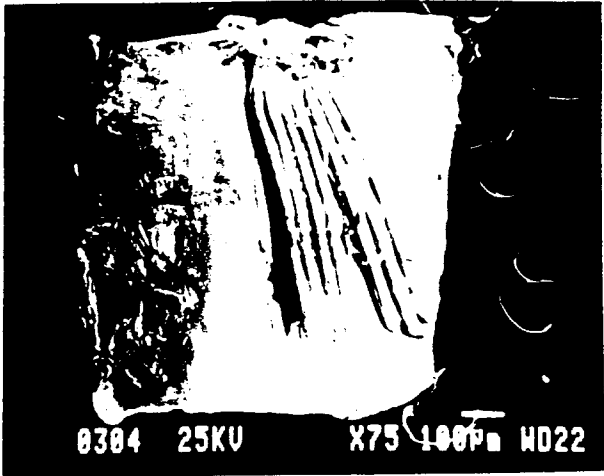


Figure 13: Histogram showing the distribution of the number of wire strands involved in a weld. The data show that most contacts were welded to the lead wire by 6-7 wire strands.

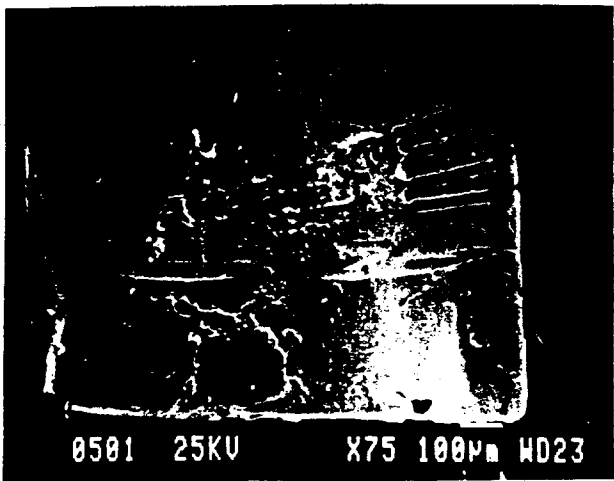
Weld Effects on Wire Strands



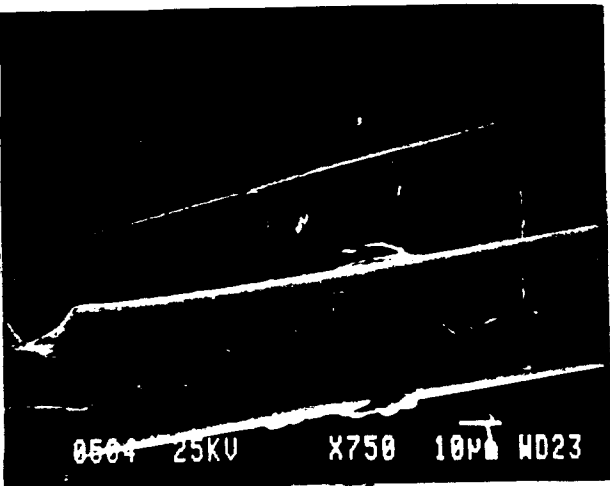
14.a: Photomicrograph of contact B.4.2



14.b: Photomicrograph of contact B.2.0



14.c: Photomicrograph of contact A.1.1



14.d: Photomicrograph of contact A.1.1

Figure 14: SEM photomicrographs representing some of the effects of the welding on the wire strands. Broken wire strands are shown in 14.a-c. The thinning of the wire strands is shown in 14.c and 14.d.

Contact with De-Bonded Weld

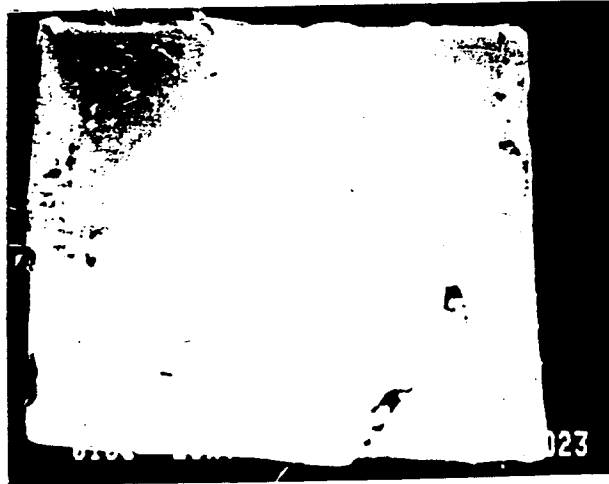


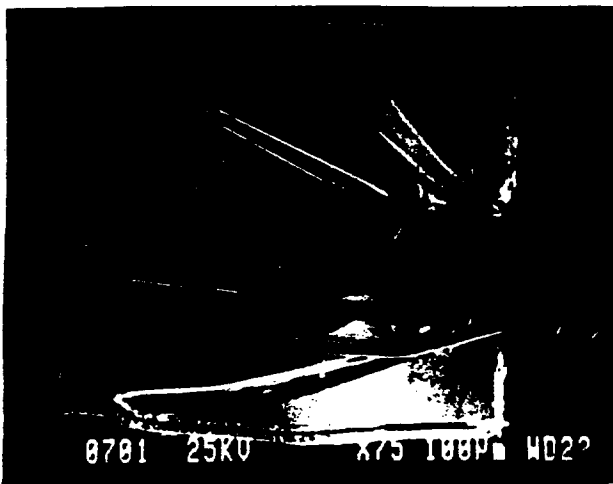
Figure 15: SEM photomicrograph of contact A.1.0. The weld debonded during extraction or cleaning of the contact. The area where the wires were is clearly visible, but no evidence of the weld can be seen on the platinum contact.

The welds differed in appearance primarily by the presence and number of voids. As presented in Figure 16.a-d, most welds were characterized by solid nuggets with a striated appearance on the surface of the welded wires. In other instances, a few voids may have been present while the overall appearance of the weld was that of a solid nugget. Distinctly different were those welds containing many voids and having a granular appearance (Figure 17.a-c). Voids can be created by escaping gas bubbles or during shrinkage as the metal solidifies. As shown in the figures, many of the voids are present in the interior of the welded region, which would support either of these origins.

In those weld nuggets containing numerous voids, the appearance of the weld nugget and the adjacent wire strands is suggestive of some corrosion. Particularly on the wire strands, apparent surface pits can be seen, as shown in Figure 17.d. While these may be corrosion pits, they are of limited frequency and size and are not readily apparent as failure sites. Wires with the appearance shown in the figure were seen in only a few other contacts. In ideal cuff fabrication, the back side of the contact should be sealed off from the *in vivo* environment by the bonded sheeting, effectively excluding the ionic path requirement for a corrosion cell. However, ineffective bonding or other inadequacies in the cuff fabrication may allow for some fluid entry into this region, making corrosion cells possible.

As was seen on the front face of some contacts and discussed in a preceding section, there were occasional defects that are likely correlated with failed weld attempts. These weld spots, as shown in Figure 18, have the appearance and shape of the weld zones with numerous voids. It seems likely that the weld electrode contacted the platinum foil directly and caused these defects.

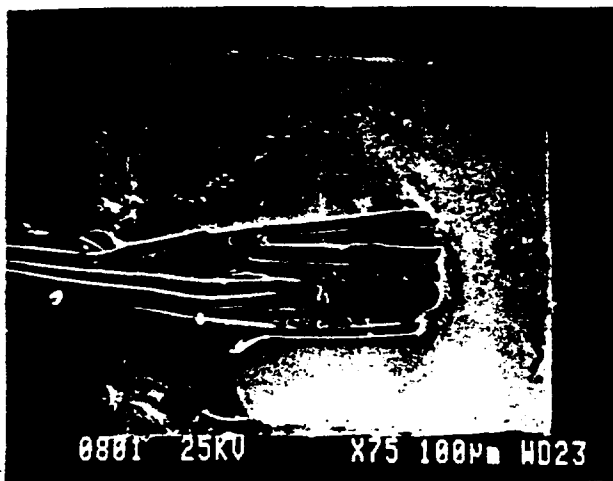
Examples of Weld Zones



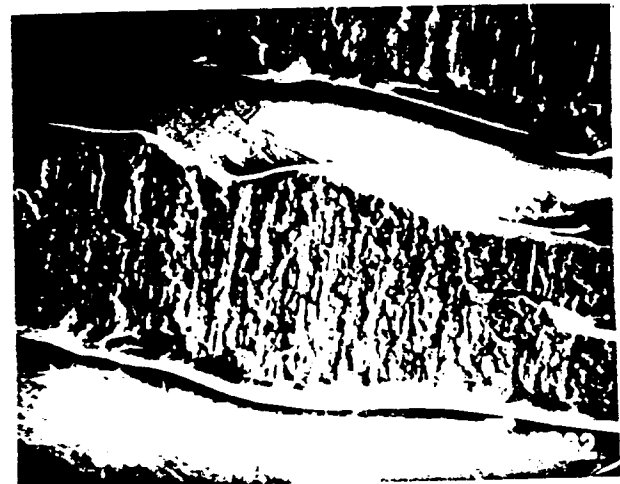
16.a: Photomicrograph of contact C.3.1



16.b: Photomicrograph of contact B.3.0



16.c: Photomicrograph of contact A.4.1



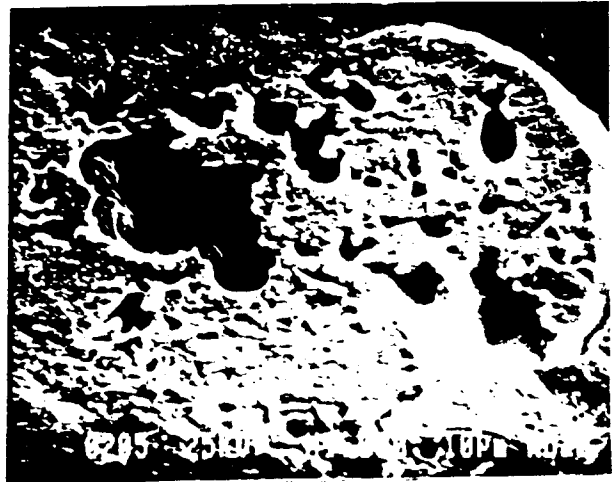
16.d: Photomicrograph of contact C.2.1

Figure 16: SEM photomicrographs representing weld zones characterized by few or no voids. The striations on the wires in the weld zone are shown clearly in the high magnification view of 16.d.

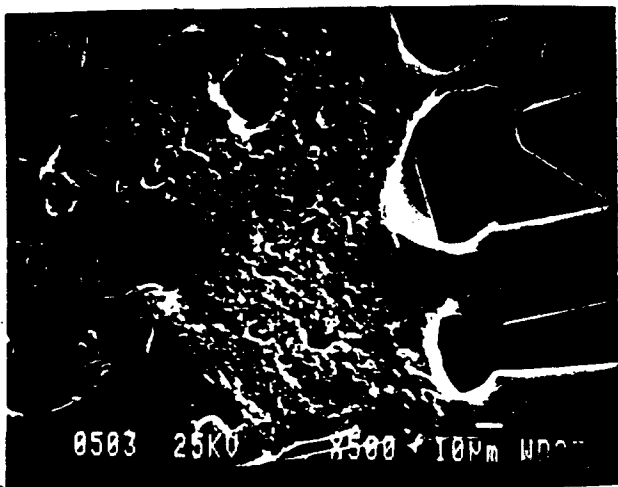
Examples of Weld Zones



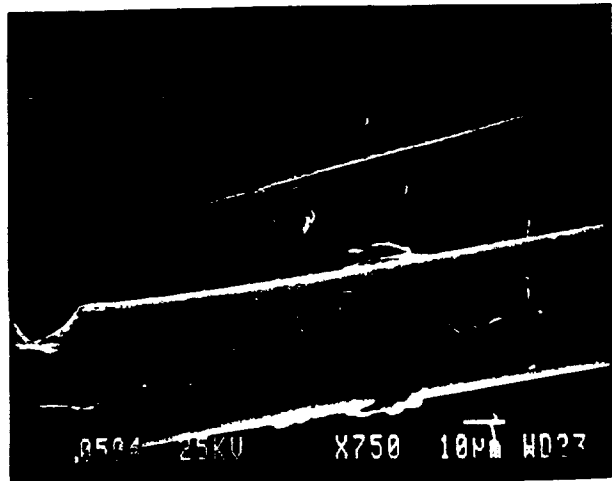
17.a: Photomicrograph of contact B.4.0



17.b: Photomicrograph of contact A.2.0



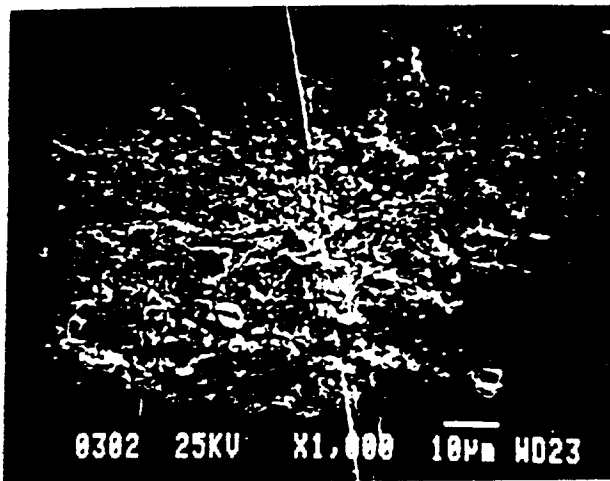
17.c: Photomicrograph of contact A.1.1



17.d: Photomicrograph of contact A.1.1

Figure 17: SEM photomicrographs weld zones with large numbers of voids and having a coarse, grainy appearance. These areas, as well as the wire strands in 17.d, are suggestive of limited corrosion.

Effects of Weld on Platinum Contacts



18.a: Photomicrograph of contact A.3.0



18.b: Photomicrograph of contact B.1.0

Figure 18: SEM photomicrographs of some metallurgical defects on the platinum contacts that were likely caused by the weld electrode.

The stainless steel lead wires are attached to the platinum foil contacts by hand produced spot welds. Variation in weld strength, position and appearance was seen on these contacts. Only four of the 36 contacts extracted from these 3 cuffs experienced weld bond failures, which would seem to indicate that the weld technique is generally sufficient to bond the wires and the contacts. However, no mechanical testing or other quantitative measures were made on these contacts to better evaluate the strength of the welds. Occasional defects were found both on the front and back faces of the contacts which can be directly correlated with welding. These defects stem primarily from inadequate welding technique, where the weld electrode was held directly to the platinum foil or where the weld electrode was applied for too long, creating both voids in the weld nugget or distortion on the front face of the platinum foil. However, the appearance, size, and location of the weld nuggets as well as the defects created by the welds were not found to correlate with any observed corrosion on the face of the exposed platinum contact.

Condition of Exposed, Stimulated Contacts

The contacts of these cuffs were stimulated at either 0, 1, 2, or 3 mA, as shown in Figure 1. In general, no differences could be found in the surface appearance of control contacts (0 mA), those contacts stimulated at 1 mA, and unexposed areas of all contacts. Occasional defects, pits and inclusions (Figure 19) were seen in all of these cases.

For those contacts stimulated at 2 and 3 mA, the surfaces of the contacts in the exposed region were found to contain a large number of pits, as shown in Figure 20. These pits are distinct from those seen in 0 and 1 mA stimulated contacts in that they are limited to the apparent exposed window region, are predominantly round, and are found in high numbers.

Charge density at the surface of electrode contacts is a concern since it has been implicated in irreversible electrochemical processes leading to corrosion, metal dissolution, and tissue damage. At the start of this study, charge densities for these contacts were calculated based on a 1 mm diameter window and were determined to be below $20\mu\text{C}/\text{cm}^2$, based on geometric area. However, the diameter of the tool used to cut the window was 0.7 mm, not the 1 mm that was used in the calculation. Based on a window size of 0.7 mm diameter and using geometric area, the charge densities were approximately 13, 26 and $39\mu\text{C}/\text{cm}^2$ for 1, 2, and 3 mA amplitudes respectively. Studies of platinum electrodes have been cited which report irreversible processes may occur at charge densities greater than $25\text{--}75\mu\text{C}/\text{cm}^2$ geometric area (Robblee and Rose, 1990).

The contact presented in Figure 20.c has a clearly delineated circular area containing pits which would seem to mark the borders of the window, even though the area is not consistent with the gouge marks. Measurement of the diameter of this circular area shows that it is not 0.7 mm, but instead is a much smaller 0.4 mm. If this represents the true size of the window, the charge density is then over $100\mu\text{C}/\text{cm}^2$. If the gouge marks on the contacts are used as the window borders, charge densities on these contacts may have ranged from 13 - $120\mu\text{C}/\text{cm}^2$.

The pitting shown on the higher amplitude stimulated contacts is certainly cause for concern. The release of corrosion products and the loss of metal mass could effect the safety and performance of implanted metal.

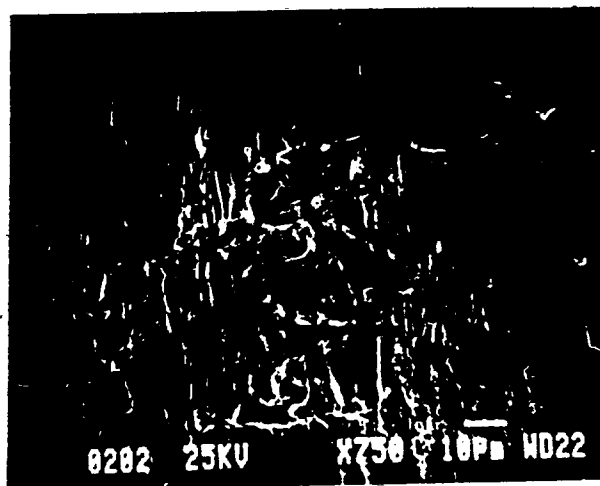
The appearance of the welds was not found to correlate with stimulation level or excessive pitting. Similarly, no correlation was found with the de-bonded welds and stimulation level. Excessive pitting was found on contacts with and without gouging by the window cutting tool.

Robblee, L.S. and T.L. Rose (1990) Electrochemical Guidelines for Selection of Protocols and Electrode Materials for Neural Stimulation. In W.F. Agnew and D.B. McCreery, eds., Neural Prostheses: Fundamental Studies, pp.25-66, Prentice-Hall, N.J.

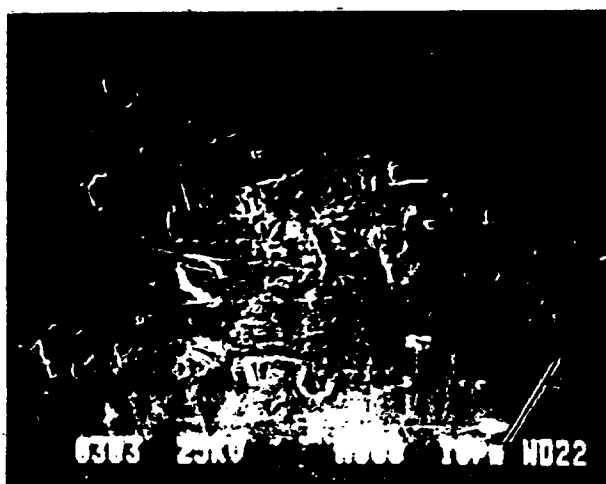
Examples of Exposed Platinum Contacts



19.a: Photomicrograph of contact C.1.2



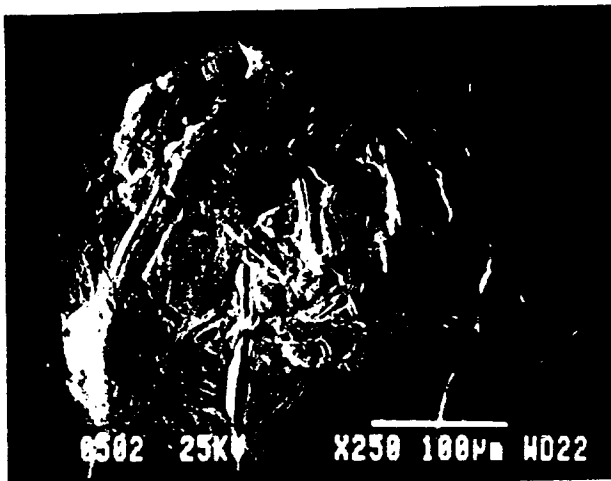
19.b: Photomicrograph of contact B.3.0



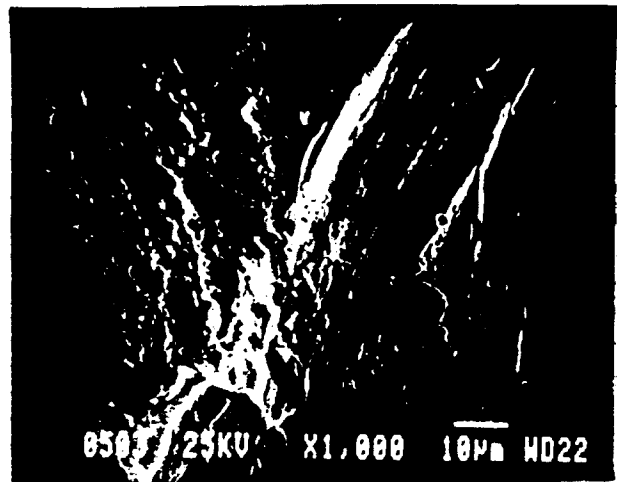
19.c: Photomicrograph of contact B.2.0

Figure 19: SEM photomicrographs representing the surface appearance in the exposed region of platinum contacts. These photos show the occasional pits and other defects found on contacts that were indistinguishable from unexposed areas of contacts.

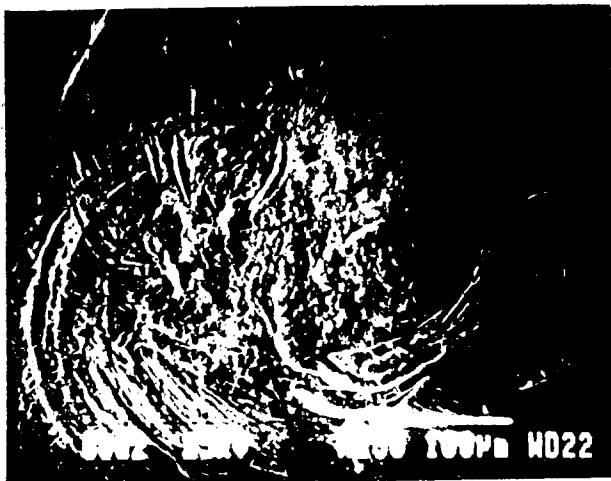
Examples of Exposed Platinum Contacts
Stimulated at 2-3 mA



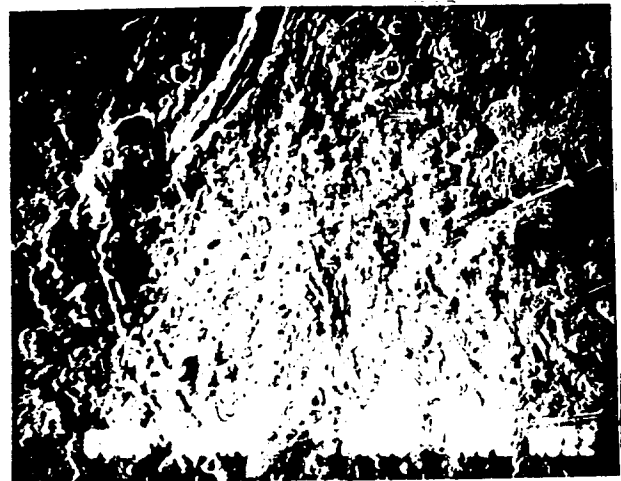
20.a: Photomicrograph of contact B.4.1



20.b: Photomicrograph of contact B.4.1



20.c: Photomicrograph of contact B.1.1



20.d: Photomicrograph of contact B.1.1

Figure 20: SEM photomicrographs of contacts stimulated at the higher amplitudes. Extensive pitting is seen in the exposed window due to high charge densities. Using the border of the pitted, circular area in 20.c as the edges of the window, the charge density exceeded $100 \mu\text{C}/\text{cm}^2$.

Conclusions and Future Work

The in vitro test regimen was performed for 10 weeks of 20Hz continuous stimulation using biphasic, balanced charge rectangular pulses. The initial cathodic phase had an amplitude of 0-3 mA with pulse duration of 50 μ s, and the secondary anodic phase had a controlled current of 0.5 mA. The observations presented above indicate that while the fabrication technique can create some damage to the contacts, including weld-related events and physical damage by the window cutting, the contacts performed without significant failures. Only at high charge densities was significant corrosion observed. It should be remembered in considering the observations discussed above that the cuffs used in these tests were rejected for in vivo use because of problems encountered in their fabrication.

Future work will involve considering the relationship between the microscopic observations discussed here and the potential measurements made during the stimulation. Additional work will include complete evaluation of contacts from cuffs implanted chronically in cats. Optimal welding technique and alternatives to welds, as well as the effects of the press curing and curl of the cuff on the platinum foil contacts will be investigated. Elemental composition analysis of the weld zones is proposed.

Section C: Quantitative Analysis of Electrode Performance in Acute and Chronic Animals

C.1.b Performance Testing in Chronic Animal Experiments

Chronic animal experiments have been performed on cats using implanted, spiral nerve cuff electrodes. The recruitment stability of these electrodes over the course of implantation has been analysed and is reported in the following manuscript, provided as Appendix I.

Appendix I

Stability of Chronically Implanted
Multiple Contact Nerve Cuff Electrodes

Warren M. Grill and J. Thomas Mortimer

(DRAFT - DO NOT DISTRIBUTE)